Ab initio study of helical silver single-wall nanotubes and nanowires

S. L. Elizondo and J. W. Mintmire
Department of Physics, Oklahoma State University, Stillwater, Oklahoma 74078, USA
(Received 1 September 2005; revised manuscript received 12 December 2005; published 26 January 2006)

We report results for the electronic structures of extended silver single-wall nanotubes (AgSWNTs) within a first-principles, all-electron self-consistent local density functional approach adapted for helical symmetry. We carried out calculations on twenty-one different AgSWNTs ranging in radii from approximately 1.3 Å to 3.6 Å. AgSWNTs with radii greater than 2.2 Å were also calculated with a silver atomic chain inserted along the nanotube axis; we refer to these composite structures as silver nanowires (AgNWs). Energetic trends for the AgSWNTs are not as predictable as expected. For example, the total energy does not necessarily decrease monotonically as nanotube radius increases, as is the case for single-wall carbon nanotubes. The conductivity of these AgSWNTs and AgNWs is also addressed. Similar to the case for helical gold nanowires, the number of conduction channels in the AgSWNTs does not always correspond to the number of atom rows comprising the nanotube. However, for all AgNWs considered, the additional silver atomic chain placed along the tube's axis results in one additional conduction channel.

DOI: 10.1103/PhysRevB.73.045431 PACS number(s): 73.22.−f, 31.10.+z, 31.15.Ew, 68.65.La

I. INTRODUCTION

As the miniaturization of electronic devices continues to advance, nanotubes and nanowires will become increasingly important in the development of these devices. A variety of procedures have been reported for constructing both gold and silver wires with nanoscale diameters.[1–10] Only one method has successfully produced gold nanowires exhibiting helical periodicity.[2,3] This unique fabrication method reported by Takayanagi and co-workers, for constructing gold nanowires with diameters as small as 0.4 nm relies on the surface reconstruction properties present in gold.[2,3,11] The *in situ* fabrication method entails using high-resolution transmission electron microscopy (HRTEM) to irradiate a gold (001) film 3 to 5 nm in thickness until holes form, creating a bridge between two holes. As this bridge narrows to less than 1.5 nm in diameter, it reconstructs into a helical nanowire suspended between two bulklike gold tips.

Rodrigues *et al.*[8] implemented the above technique[2,3] using silver. They successfully synthesized silver nanowires exhibiting a tube-like contrast pattern with an especially stable atomic structure. Although the silver wires were produced with diameters comparable to the gold nanowires reported by Takayanagi and co-workers,[2,3] the silver wires did not undergo a surface reconstruction phase leading to the helical structure observed for gold nanowires. However, a different fabrication method, one that does not rely directly upon surface reconstruction, may successfully yield silver nanowires exhibiting helical periodicity. For example, Hong *et al.*,[5] synthesized single-crystalline silver nanowires in an ambient solution phase. These silver nanowires, with 0.4 nm diameter, are comparable to the $(4,2)$ silver nanowire discussed here with an energetic local minima. The structure of this silver nanowire is markedly different than bulk, and although not immediately apparent, this structure does exhibit helical periodicity.

Nevertheless, we are particularly interested in the helical multishell nanowires and a helical single-wall gold nanotube synthesized by Takayanagi and co-workers,[2,3] which are favorable structures for our method of calculation based on the use of helical symmetry. As a starting point, we decided to model silver instead of more complex systems involving gold. Calculations for gold require treating relativistic effects, which is beyond the capability of our current first-principles approach. In this preliminary work, we will address similar trends in our results compared with theoretical work using gold and silver described elsewhere.[12–18]

The single-wall gold nanotube and the smallest multishell gold nanowire reported experimentally[2,3] have been studied theoretically by others.[8,13–16] Calculations on several gold nanotube structures published elsewhere report results in terms of energy per unit length of wire, defined by the positive work done in drawing the wire out of the bulklike gold tips, denoted as the string tension.[12,14] Based upon first-principles calculations, Senger *et al.* studied a variety of possible structures for gold single-wall nanotubes.[14] In addition to the (5,3) gold nanotube fabricated experimentally,[3] they calculated six additional single-walled nanotubes as either tip-suspended or free-standing structures. The (5,5) tube was determined to be the most energetically favorable free-standing single-wall gold nanotube, and they predicted one other tube, the tip-suspended (4,3), as another energetically favorable single-wall gold nanotube yet to be observed experimentally.[14] First-principles calculations by Yang showed that the (5,3) gold nanotube was capable of enduring large elongation without a change in conductivity.[15] Perhaps the most interesting theoretical analysis is a recent first-principles study of the smallest helical multishell gold nanowire, a single-wall gold nanotube with an inserted chain, in which the authors conclude that helical gold nanowires are good candidates for nanometer-scale solenoids.[16]

The conductivity of the related gold nanowires[14–16] and very thin silver nanowires[17,18] has been addressed in other theoretical studies. It is of interest due to the observation of quantized conductance in both gold and silver nanowires.[1,8] Ohnishi *et al.* observed quantized conductance through individual rows of tip-suspended gold atoms.[1] The conductance

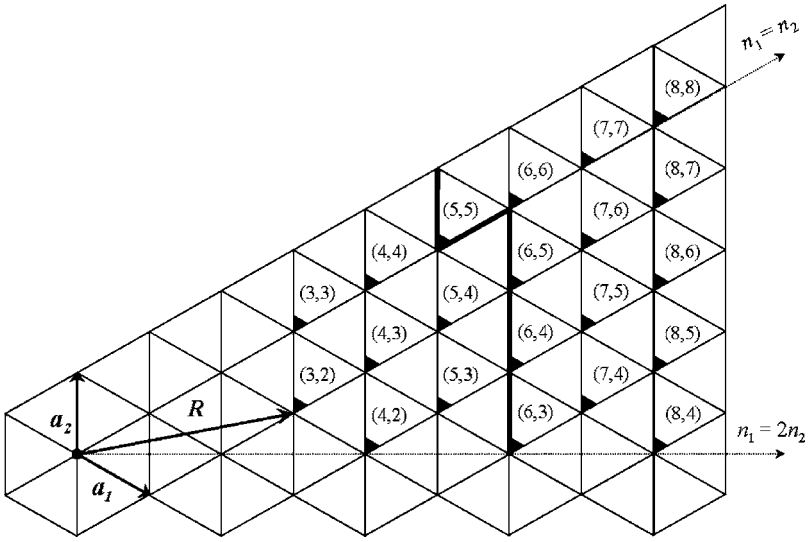

FIG. 1. Triangular network of silver (or gold) atoms. Basis vectors are designated as $\boldsymbol{a}_1$ and $\boldsymbol{a}_2$. Each tube is labeled by two integers (n_1,n_2), where the rollup vector is $\boldsymbol{R}=n_1\boldsymbol{a}_1+n_2\boldsymbol{a}_2$. The dashed lines represent lines of symmetry; an irreducible wedge is formed between the lines $n_1=n_2$ and $n_1=2n_2$. AgSWNTs labeled with a solid marker correspond to the nanotubes that we consider in the present study. AgSWNTs located to the right of the bold line, ranging from (5,5) to (8,4), were also modeled with a silver atomic chain inserted along the axis of the nanotube. AgSWNTs containing an axial chain are designated as nanowires (AgNWs).

was observed in units of $G_0=2e^2/h$, where e is the electron charge and h is Planck's constant. With each gold atomic chain contributing one channel of conductance, the quantized conductance for a N-channel system is expressed as N_cG_0. Consistent with this interpretation, the conductance is quantized such that it increases by a quantum conductance $2e^2/h$ whenever a band crosses the Fermi level.[19,20] For an individual atomic chain, only one conductance channel (i.e., $N_c=1$) or band crosses the Fermi level. Within the (n_1,n_2) notation scheme used herein, described in detail in Sec. II, n_1 is equal to the number of helical strands comprising the tube. Because helical gold nanowires are essentially comprised of n_1-atom strands winding about the wire axis, the natural question to ask is whether quantized conductance is observed in steps of n_1G_0 in the helical nanotubes and nanowires. Other studies have found that the number of bands crossing the Fermi level, or the number of putative conduction channels, do not always correspond to the numbers of atom rows in the helical gold nanowires.[12,14–16] Similar studies have addressed the quantum transport mechanism present in silver nanowires.[17,18]

II. APPROACH

Modeling the silver nanotubes involves "rolling up" a triangular sheet of silver atoms and mapping the atoms onto the surface of a cylinder, comparable to rolling up a graphite sheet for a carbon nanotube. For the triangular sheet depicted in Fig. 1, each Bravais lattice vector $\boldsymbol{R}$ is defined by two primitive lattice vectors $\boldsymbol{a}_1$ and $\boldsymbol{a}_2$ and the pair of integers (n_1,n_2), so that the lattice vector

$$\boldsymbol{R}=n_1\boldsymbol{a}_1+n_2\boldsymbol{a}_2. \tag{1}$$

The radius for an (n_1,n_2) nanotube is given by

$$\rho=\frac{|\boldsymbol{R}|}{2\pi}=\frac{d}{2\pi}\sqrt{n_1^2+n_2^2-n_1n_2}, \tag{2}$$

where d is the Ag-Ag bond length from the triangular sheet. The notation chosen here is consistent with the notation used elsewhere[2,3,12–15] and is related to the convention used for carbon nanotubes. As shown in Fig. 1, a line of symmetry extends through the triangular lattice for $n_1=n_2$, and another line of symmetry is present for $n_1=2n_2$. All possible AgSWNTs can be reduced by symmetry to an irreducible wedge formed between the two lines of symmetry. Analogous to carbon nanotubes, each $\boldsymbol{R}$ within this wedge defines a different AgSWNT, and all unique AgSWNTs defined by rolling up the triangular sheet of silver atoms can be generated by this set of $\boldsymbol{R}$'s.[21]

We have investigated the electronic structure of AgSWNTs using a first-principles, all-electron self-consistent local density functional (LDF) approach adapted for helical symmetry. A 3-21G basis set was used, along with 512 k points in the central Brillioun zone. The approach used here has been discussed in detail elsewhere.[22–24] We define the helical periodicity of the silver nanotubes in terms of a unit cell of a small number of silver atoms and a screw operation $S(h,\phi)$ that will generate the lattice of nanotube nuclear coordinates. For mathematical convenience, we define the screw operation in terms of a translation h units down the z axis in conjunction with a right-handed rotation ϕ about the

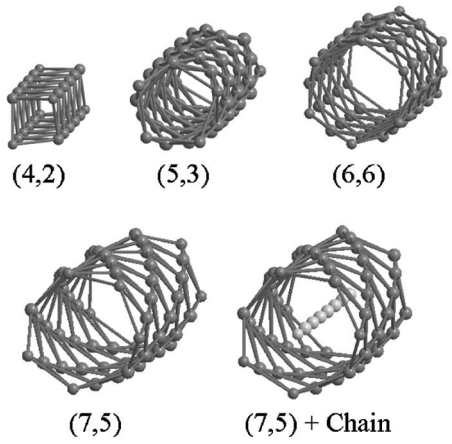

FIG. 2. Models of selected AgSWNTs and the (7,5) AgNW (AgSWNT + inserted silver atomic chain).

TABLE I. Total energies relative to the (7,5) AgNW. The structures are listed by increasing radii, and N_{Ag} represents the number of silver atoms per unit cell. Super cells were used for the AgNWs to match the periodicity of the chains with their respective AgSWNTs.

		AgSWNT		AgNW (AgSWNT+Center Chain)	
Structure	Radius (Å)	N_{Ag}	eV/N_{Ag}	N_{Ag}	eV/N_{Ag}
(3,2)	1.3096	1	0.8956		
(3,3)	1.4801	3	0.9430		
(4,2)	1.6099	2	0.4911		
(4,3)	1.6756	1	0.5488		
(4,4)	1.8398	4	0.5528		
(5,3)	1.9972	1	0.4448		
(5,4)	2.0640	1	0.4794		
(5,5)	2.2361	5	0.4671	6	0.3772
(6,3)	2.3156	3	0.4251	7	0.3817
(6,4)	2.3497	2	0.4443	7	0.3156
(6,5)	2.4812	1	0.4640	7	0.0994
(6,6)	2.6834	6	0.4668	7	0.0014
(7,4)	2.7300	1	0.4173	8	0.0015
(7,5)	2.8029	1	0.4158	8	0.0000
(7,6)	2.9431	1	0.4272	8	0.0554
(8,4)	3.0874	4	0.4158	9	0.0446
(8,5)	3.1306	1	0.3945	9	0.0634
(7,7)	3.1417	7	0.4491	8	0.1022
(8,6)	3.2250	2	0.4250	9	0.0795
(8,7)	3.3524	1	0.3857	10	0.1212
(8,8)	3.5523	8	0.4006	9	0.1610

z axis. Because the symmetry group generated by the screw operation S is isomorphic with the one-dimensional translation group, Bloch's theorem can be generalized so that the one-electron wave functions will transform under S according to

$$S^m \psi_i(\boldsymbol{r};\kappa) = \sum_j c_{ji}(\kappa)\varphi_j(\boldsymbol{r};\kappa). \tag{3}$$

The quantity κ is a dimensionless quantity which is conventionally restricted to a range of $-\pi < \kappa \leqslant \pi$, a central Brillouin zone. The one-electron wave functions ψ_i are constructed from a linear combination of Bloch functions φ_j, which are in turn constructed from a linear combination of nuclear-centered Gaussian-type orbitals $\chi_j(\boldsymbol{r})$

$$\psi_i(\boldsymbol{r};\kappa) = \sum_j c_{ij}(\kappa)\varphi_j(\boldsymbol{r};\kappa), \tag{4}$$

$$\varphi_j(\boldsymbol{r};\kappa) = \sum_m \exp(-i\kappa m) S^m \chi_j(\boldsymbol{r}). \tag{5}$$

The silver single-wall nanotubes simulated in the present study are indicated in Fig. 1 by solid tick marks, and selected models for the respective silver single-wall nanotubes (AgSWNTs) are shown in Fig. 2. All structures were calculated at or near equilibrium conformation. The specific tubes were chosen based on theoretical work published elsewhere for gold systems,[14,15] as well as the single-wall gold nanotube fabricated in Ref. 3.

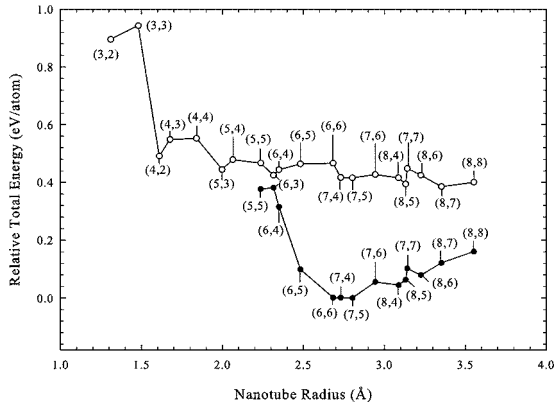

FIG. 3. Total energy per silver atom versus nanotube radius. Open circles represent AgSWNTs and closed circles represent AgNWs. The (7,5) AgNW has the lowest energy and is centered about zero; the energies of all other tubes are plotted with respect to zero. Local minima in total energy are shown for the (4,2), (5,3), (6,3), (7,4), (7,5), (8,5), and (8,7) AgSWNTs.

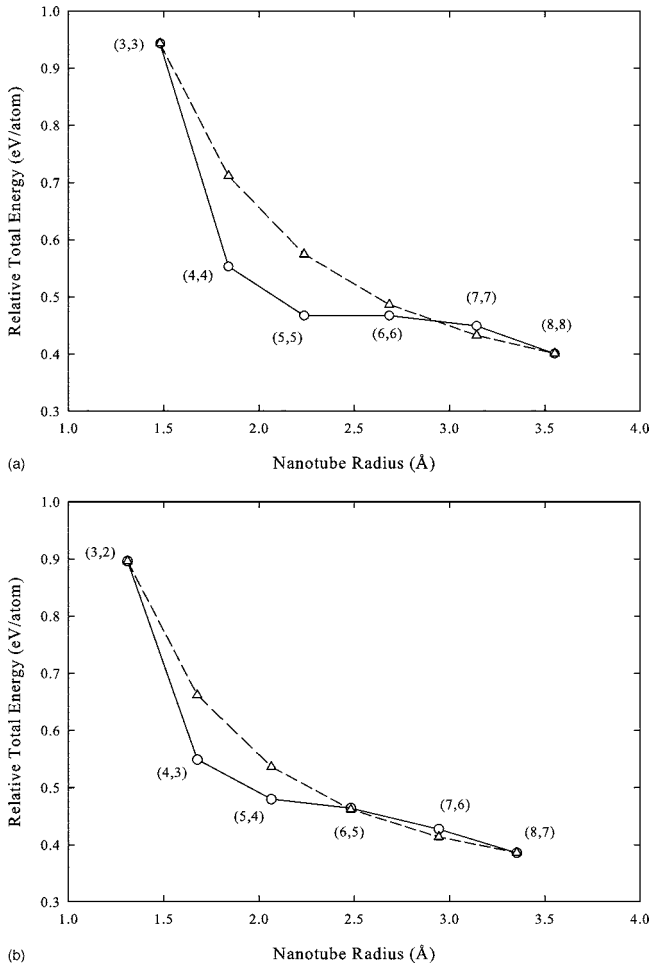

FIG. 4. Total energy per silver atom versus nanotube radius for all (a) "$n_1=n_2$" type and (b) "$n_1=n_2+1$" type AgSWNTs. The solid line represents calculated values, while the dashed line represents a $1/R^2$ fit. In each case, the calculated values fall off at a rate faster than $1/R^2$. Calculated values are given in Table I.

AgSWNTs with radii greater than 2.2 Å were also calculated with a silver atomic chain inserted along the axis of the nanotube—these structures are termed silver nanowires (AgNWs). The model for the (7,5) AgNW is shown in Fig. 2. The bond lengths of the inserted chains range from 2.43 Å to 2.88 Å and were chosen in order to match the periodicity of the respective nanotube. The atomic chain with the lowest total energy in this study had a bond length of 2.61 Å, which is comparable to the 2.64 Å optimized bond length recently reported by Agrawal *et al.*[18] for a monatomic linear silver chain. On average, the total energies of the chains are approximately 0.04 eV higher than the (3,3) AgSWNT, the structure with the highest total energy.

III. RESULTS

The optimized total energies for the AgSWNTs and AgNWs are given with respect to radius in Table I and are plotted in Fig. 3. As a result of our calculations, we find local minima in total energy to exist for the (4,2), (5,3), (6,3), (7,4), (7,5), (8,5), and (8,7) AgSWNTs. Upon inserting the chain into the (7,5) nanotube, this structure becomes the most energetically favorable AgNW, with the (6,6) and (7,4) AgNWs following within 10^{-4} eV. We find the (3,2) and (3,3) to be the highest in total energy and, therefore, the least favorable structures within this study.

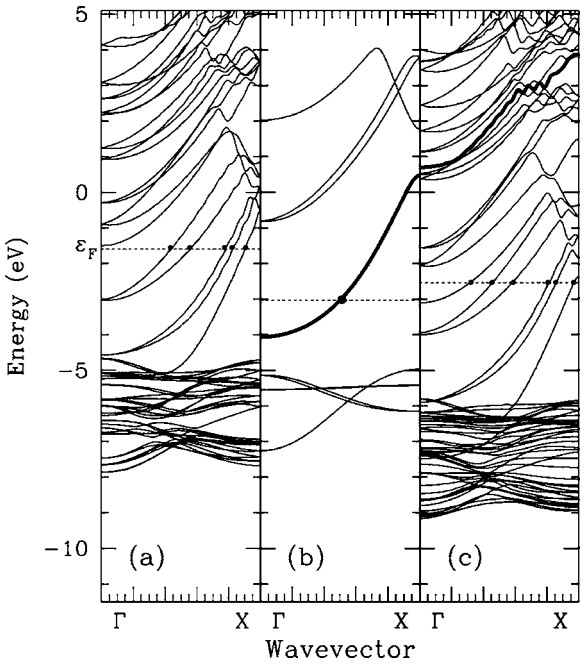

FIG. 5. Band structures for the (a) (7,4) AgSWNT, (b) silver atomic chain, and (c) the (7,4) AgNW. Fermi levels are shown with a dashed line. Points correspond to the orbital density images shown in Fig. 6. The band crossing the Fermi level in (b), shown in bold, is shifted higher in energy into the conduction band in (c). The band that lies just above the Fermi level in the AgSWNT shown in (a) dips below the Fermi level upon inserting the chain as shown in (c). Inserting the chain lowers the energies of the bands from the AgSWNT with respect to the Fermi level, resulting in one additional conduction channel. The number of Fermi crossings corresponds to the number of conduction channels in a particular structure. There are five Fermi crossings in (a), one Fermi crossing in (b), and six Fermi crossings in (c).

Energetic trends for the AgSWNTs with respect to nanotube radius differ from what we would expect; the total energy does not necessarily decrease monotonically as radius increases. In some cases, between local minima, the total energy per silver atom increases as nanotube radius increases. Elastic strain models, such as those used for carbon SWNTs, would predict that the total strain energy should increase as the radius decreases.[25,26] The strain energy per carbon atom in carbon nanotubes relative to an unstrained graphite sheet scales as $1/R^2$ (where R is the tube's radius).[27] A smooth $1/R^2$ trend is not present within our results for the AgSWNTs. If we group the AgSWNTs by their geometries, the total energy versus radius curve becomes smoother, but we see a trend where the calculated energy initially falls off at a rate faster than $1/R^2$. We grouped the applicable (n_1,n_2) AgSWNTs as belonging to either the $n_1=n_2$ group [i.e., the (5,5) AgSWNT] or the $n_1=n_2+1$ group [i.e., the (5,4) AgSWNT]. The plots for the $n_1=n_2$ and $n_1=n_2+1$ groups are given in Figs. 4(a) and 4(b), respectively. Although there are

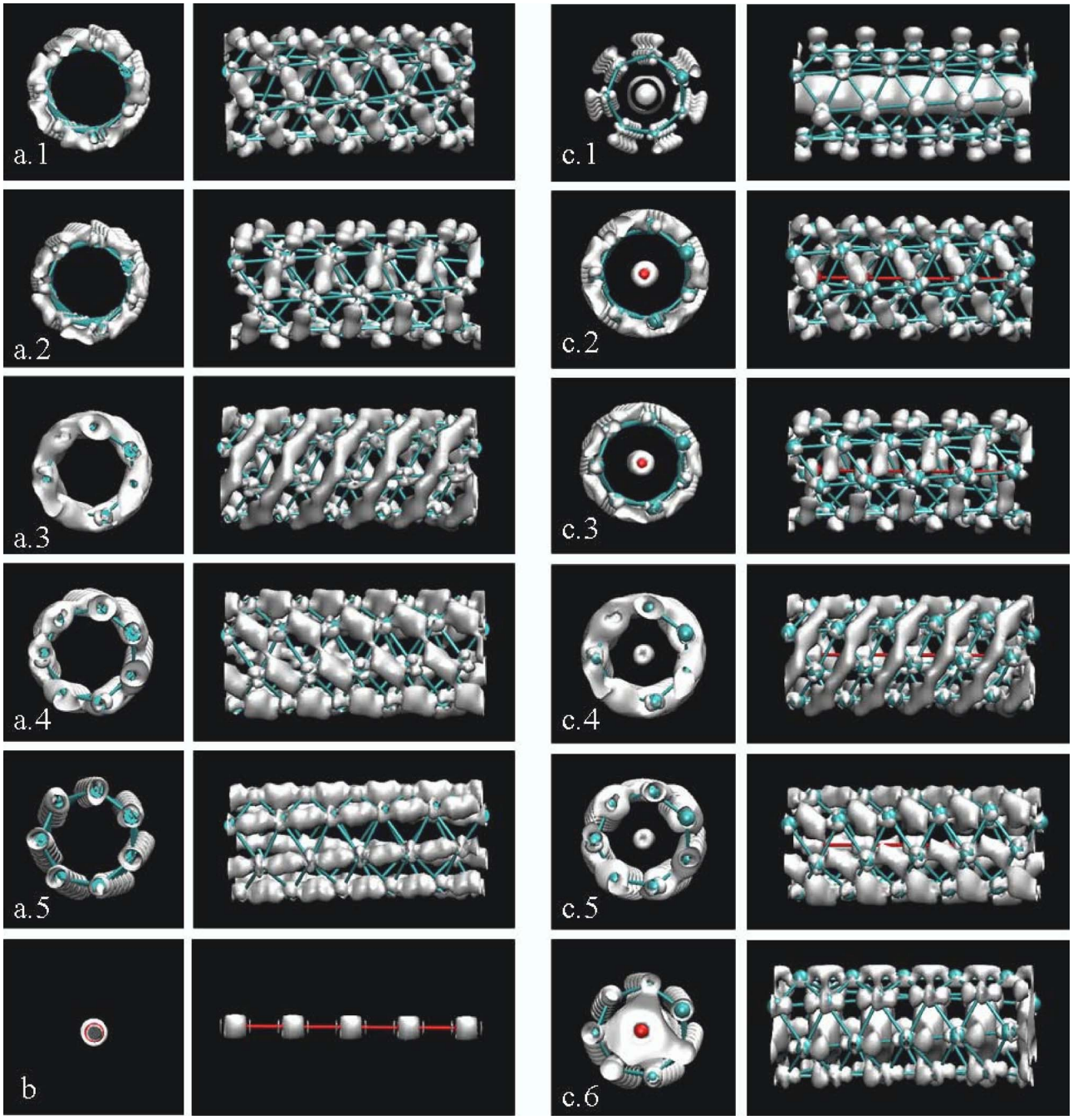

FIG. 6. (Color online) Orbital densities for the (a) (7,4) AgSWNT, (b) silver atomic chain, and (c) (7,4) AgNW. The structure of the inserted chain (c) is shown in red to aid in visualization. The images correspond to bands at specific points within the Brillioun zone, as indicated in Fig. 5 by solid dots. The numbering scheme from 1 to 6 corresponds to the solid dots located from left to right, respectively.

two additional groups present, the $n_1=n_2+2$ and the $n_1=n_2+3$ group, these later two groups do not contain AgSWNTs with small enough diameters to see the trend—their curves are essentially flat.

Although the number of conduction channels in a AgSWNT does not always correspond to the number of atom rows, inserting an atomic chain along the nanotube axis always contributes one additional conduction channel. Again, for the (n_1,n_2) notation scheme chosen here, n_1 is equal to the number of helical strands comprising the tube. The band structures from our calculations are shown in Fig. 5 for the (7,4) AgSWNT, the silver atomic chain, and the (7,4) with the inserted chain. The (7,4) AgNW corresponds to the smallest multishell gold nanowire found experimentally[2] and has recently been suggested as a possible nanosolenoid.[16] The inserted atomic chain contributes one conduction channel, while the (7,4) tube without an inserted chain with $n_1=7$, contributes five conduction channels. The composite structure with $n_1=8$ has six conduction channels. These results agree with results for the number of conduction channels from first-principles calculations on the 7–1 helical gold nanowires.[12,16] We note, however, that our results are some-

what dependent on the basis set. In earlier work using an STO-3G basis set,[23] we did not find the same number of conduction channels as discussed above. We concluded, however, that the STO-3G basis set was not sufficient for modeling silver. We believe that our current results with the 3-21G basis set are more reliable.

The orbital densities for the (7,4) AgSWNT, inserted silver atomic chain, and (7,4) AgNW are shown in Fig. 6. The images correspond to bands at specific points within the Brillioun zone, depicted in Fig. 5 by solid dots. The numbering scheme in Fig. 6 corresponds to these points located from left to right, respectively. Upon close inspection of the band structures, we note that the band crossing the Fermi level in Fig. 5(b) from the chain alone does not correspond directly to the extra band crossing the Fermi level in Fig. 5(c). Rather, the band lying just above the Fermi level in the AgSWNT shown in Fig. 5(a) dips below the Fermi level upon inserting the chain, as shown in Fig. 5(c). Inserting the chain lowers the energies of the bands from the AgSWNT with respect to the Fermi level, resulting in one additional conduction channel. The bands mix and introduce substantial chain character into multiple bands near the Fermi level. The band crossing the Fermi level in Fig. 5(b) does not simply disappear—it is shifted higher in energy into the conduction band. This behavior upon inserting the chain consistently results in an extra conduction channel for all AgNWs considered in this study.

We observe the following for all AgSWNTs considered here: three conduction channels are present if $n_1=3$ or 4, five conduction channels are present if $n_1=5,6$, or 7, and seven conduction channels are present if $n_1=8$. In agreement with Senger *et al.*,[14] our band structure calculations for the (5,3), (5,4), and (5,5) AgSWNTs with $n=5$ silver atom strands, all have densities of states corresponding to five conduction channels. In agreement with other theoretical work, the structure corresponding to the (4,2) AgSWNT with $n_1=4$ helical strands exhibits three conductance channels.[16,17]

IV. SUMMARY

We have carried out first-principles calculations on extended silver single-wall nanotubes and nanowires. After providing an overview of the structural identification of these AgSWNTs and AgNWs, we discussed energetically favorable structures and examined the conductivity. We found local minima in total energy for the (4,2), (5,3), (6,3), (7,4), (7,5), (8,5), and (8,7) AgSWNTs. Out of all the AgSWNTs and AgNWs studied here, the (7,5) AgNW is the most energetically favorable structure. While the number of conductional channels in a AgSWNT does not always correspond to the number of atom rows comprising the nanotube, inserting a silver atomic chain along the axis of the nanotube results in one additional conductance channel.

ACKNOWLEDGMENTS

This work was supported by the ONR, the DoD HPCMO CHSSI program, the NSF Oklahoma EPSCoR NanoNet, and the NSF IGERT program at OSU.

[1] H. Ohnishi, Y. Kondo, and K. Takayanagi, Nature (London) **395**, 780 (1998).
[2] Y. Kondo and K. Takayanagi, Science **289**, 606 (2000).
[3] Y. Oshima, A. Onga, and K. Takayanagi, Phys. Rev. Lett. **91**, 205503 (2003).
[4] M. Watanabe, H. Minoda, and K. Takayanagi, Jpn. J. Appl. Phys., Part 1 **43**, 6347 (2004).
[5] B. H. Hong, S. C. Bae, C. Lee, S. Jeong, and K. S. Kim, Science **294**, 348 (2001).
[6] N. Nilius, T. M. Wallis, and W. Ho, Science **297**, 1853 (2002).
[7] T. M. Wallis, N. Nilius, and W. Ho, Phys. Rev. Lett. **89**, 236802 (2002).
[8] V. Rodrigues, J. Bettini, A. R. Rocha, L. G. C. Rego, and D. Ugarte, Phys. Rev. B **65**, 153402 (2002).
[9] Y. Xiong, Y. Xie, C. Wu, J. Yang, Z. Li, and F. Xu, Adv. Mater. (Weinheim, Ger.) **15**, 405 (2003).
[10] Q. Zhao, J. Qiu, C. Zhao, L. Hou, and C. Zhu, Chem. Lett. **34**, 30 (2005).
[11] R. H. M. Smit, C. Untiedt, A. I. Yanson, and J. M. van Ruitenbeek, Phys. Rev. Lett. **87**, 266102 (2001).
[12] E. Tosatti, S. Prestipino, S. Kostlmeier, A. Dal Corso, and F. D. Di Tolla, Science **291**, 288 (2001).
[13] A. Hasegawa, K. Yoshizawa, and K. Hirao, Chem. Phys. Lett. **345**, 367 (2001).
[14] R. T. Senger, S. Dag, and S. Ciraci, Phys. Rev. Lett. **93**, 196807 (2004).
[15] Chih -Kai Yang, Appl. Phys. Lett. **85**, 2923 (2004).
[16] T. Ono and K. Hirose, Phys. Rev. Lett. **94**, 206806 (2005).
[17] J. Zhao, C. Buia, J. Han, and J. P. Lu, Nanotechnology **14**, 501 (2003).
[18] B. K. Agrawal, S. Agrawal, and S. Singh, J. Nanosci. Nanotechnol. **5**, 635 (2005).
[19] B. J. van Wees, H. van Houten, C. W. J. Beenakker, J. G. Willamson, L. P. Kouwenhoven, D. van der Mavel, and C. T. Foxon, Phys. Rev. Lett. **60**, 848 (1988).
[20] E. Tekman and S. Ciraci, Phys. Rev. B **43**, 7145 (1991).
[21] C. T. White and J. W. Mintmire, J. Phys. Chem. B **109**, 52 (2005).
[22] J. W. Mintmire, in *Density Functional Methods in Chemistry*, edited by J. K. Labanowski (Springer-Verlag, Berlin, 1990), pp. 125–138.
[23] M. S. Miao, P. E. Van Camp, V. E. van Doren, J. J. Ladik, and J. W. Mintmire, Phys. Rev. B **54**, 10430 (1996).
[24] S. L. Elizondo and J. W. Mintmire, Int. J. Quantum Chem. **105**, 772 (2005).
[25] G. G. Tibbetts, J. Cryst. Growth **66**, 632 (1984).
[26] J. S. Speck, M. Endo, and M. S. Dresselhaus, J. Cryst. Growth **94**, 834 (1989).
[27] D. H. Robertson, D. W. Brenner, and J. W. Mintmire, Phys. Rev. B **45**, R12592 (1992).